ACS OMEGA

Article

Cite This: ACS Omega 2018, 3, 5355−5361

Rapid Determination of Acetic Acid, Furfural, and 5-Hydroxymethylfurfural in Biomass Hydrolysates Using Near-Infrared Spectroscopy

Jun Li,[†] Meng Zhang,[‡] Floyd Dowell,*[,§] and Donghai Wang*[,†]

[†]Department of Biological and Agricultural Engineering and [‡]Department of Industrial and Manufacturing Systems Engineering, Kansas State University, Manhattan, Kansas 66506, United States

[§]Center for Grain and Animal Health Research, USDA, Agricultural Research Service, 1515 College Avenue, Manhattan, Kansas 66502, United States

ABSTRACT: Near-infrared spectroscopy (NIRS) is a rapid detection technique that has been used to characterize biomass. The objective of this study was to develop suitable NIRS models to predict the acetic acid, furfural, and 5-hydroxymethylfurfural (HMF) contents in biomass hydrolysates. Using a uniform distribution of pretreatment conditions, 60 representative biomass hydrolysates were prepared. Partial least-squares regression was used to develop models capable of predicting acetic acid, furfural, and HMF contents. Optimal models were built using the wavenumber range of 9000−8000 and 7000−5000 cm^{-1} with high R^2 for calibration and validation models, small root-mean-square error of calibration (<0.21) and root-mean-square error of prediction (RMSEP, <0.42), and a ratio of the standard deviation of the reference values to the RMSEP of >2.7. The NIRS method largely reduced the analytical time from ∼55 to <1 min and has no cost for reagents.

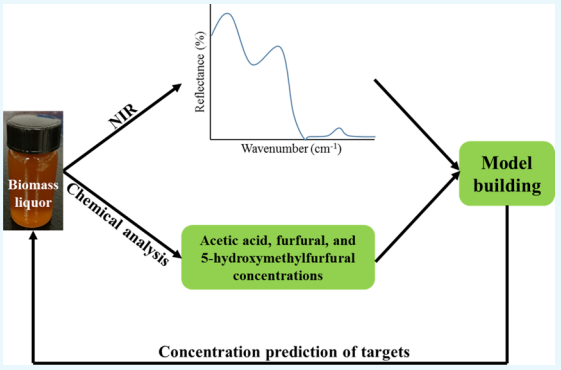

1. INTRODUCTION

Developing low-cost and highly efficient alternative renewable energy to ease our energy resource challenges and air pollution is a common goal for researchers working in the field of energy. Bioethanol derived from biomass is a desirable alternative to conventional petroleum-based fossil fuels and has received widespread attention.[1,2] Although starch-based crops, such as corn, sorghum, and wheat, have a high ethanol titer and yield, their annual supply for ethanol production is quite finite because of the competition with human food and animal feed.[3] The biofuel sector has been struggling to overcome the "food vs fuel" controversy due to the limited natural resources, particularly the limited productive agricultural lands and usable freshwater. Thus, nonfood lignocellulosic biomass, such as corn stover, switchgrass, sorghum stalks, miscanthus, big bluestem, and agricultural residues, provides a potentially valuable resource to produce ethanol because of its renewability and availability at low cost.[4,5] Unlike that of starch-based crops, however, the use of lignocellulosic biomass for ethanol production only through saccharification and fermentation is not feasible under current technical conditions because of its complex nature.[6,7] Pretreatment is an essential step to disrupt biomass microstructures and cleave the chemical linkages among cellulose, hemicellulose, and lignin, which are three major components of lignocellulosic biomass.[5,8]

In recent years, a variety of pretreatment methods for lignocellulosic biomass have been proposed, but most of them are still in the laboratory-scale exploration stage and only very few have been applied in the bioethanol industry. At present, the liquid hot water pretreatment method has also received much attention because of zero chemical use in the pretreatment process, as compared with the industrialized dilute sulfuric acid pretreatment method.[9−11] High-temperature treatment is employed in both methods. High-temperature acid pretreatment causes the chemical structures of biomass to be disrupted and release monosaccharides; however, it also causes the degradation of sugar monomers to furfural and 5-hydroxymethylfurfural (HMF). The acetic group on hemicellulose branches is released during pretreatment and acidizes the biomass slurry, which also causes the degradation of sugar to furfural and HMF.[12] Furfural is obtained from pentose degradation and HMF from hexose degradation.[13,14] The formation of furfural and HMF causes fermentable sugar loss and inhibits the downstream enzyme and yeast activities especially at high solid loading hydrolysis and fermentation, thus lowering the final ethanol yield.[15] Therefore, it is necessary to determine the concentrations of furfural, HMF, and acetic acid in treated biomass hydrolysates (Tables 1 and 2).

Currently, the most common method for furfural, HMF, and acetic acid detection in biomass hydrolysates is the high-performance liquid chromatography (HPLC) method recommended by the National Renewable Energy Laboratory

Received: April 3, 2018
Accepted: May 8, 2018
Published: May 18, 2018

DOI: 10.1021/acsomega.8b00636
ACS Omega 2018, 3, 5355−5361

Table 1. Experimental Design of Biomass Pretreatment[a]

sample (g)	sulfuric acid concentration (wt %)	sulfuric acid volume (mL)	temperature (°C)	time (min)
5.0	0	50	190	30
5.0	0	50	210	20
5.0	0	50	210	30
5.0	0	50	230	10
5.0	0	50	230	20
5.0	0	50	230	30
5.0	5	50	120	30
5.0	5	50	120	60
5.0	5	50	140	30
5.0	2	50	165	20
5.0	2	50	165	30
5.0	2	50	190	30
5.0	0.5	50	210	10
5.0	0.5	50	210	20
5.0	0.5	50	210	30

[a]All four types of biomass (corn stover, switchgrass, sorghum, and miscanthus) followed the experimental design above.

(NREL). The HPLC method uses an organic acid column and a universal refractive index detector (RID) as the separation and detection units, respectively, with a running time up to 50−55 min.[16] Subsequently, some other methods[17−22] based on liquid and gas chromatography and mass spectrometry techniques have been proposed. These methods are time-consuming and expensive and also require skilled operators. Thus, it is essential to develop a rapid and low-cost detection method for furfural, HMF, and acetic acid in biomass hydrolysates. Near-infrared spectroscopy (NIRS) is a widely investigated analytical tool and has been applied in quality control and process monitoring of food, pharmaceutical, and agricultural industries because of the advantages of being nondestructive; thus, samples can be reused, requiring no reagents that can harm the sample or the environment, short detection time, and low detection cost over the traditional laboratory methods.[23−27] Xu et al.[28] developed NIRS prediction models for sugar contents in corn stover hydrolysates with the coefficient of determination (R^2) of 0.89, the root-mean-square error of prediction (RMSEP) of 1.08 g/L, and the ratio of the standard deviation (SD) of reference data to RMSEP (RPD) of 2.76 for glucose; R^2 of 0.83, RMSEP of 1.60 g/L, and RPD of 2.23 for xylose; and R^2 of 0.75, RMSEP of 0.53 g/L, and RPD of 1.51 for arabinose. Some NIRS models have also been developed for the prediction of structural sugars, lignin, and extractives in biomass and are very useful as a screening tool to select desirable strains from numerous blind samples.[29−34] Also, some NIRS models have been developed to predict the heating value, elemental compositions, and moisture and ash contents of biomass with satisfactory R^2 and RMSEP.[35−37]

To date, no study has investigated the potential of NIRS spectroscopy to predict the contents of furfural, HMF, and acetic acid in biomass hydrolysates. Thus, the objective of this work was to develop a rapid and low-cost quantitative method using NIRS spectroscopy for the determination of furfural, HMF, and acetic acid in biomass hydrolysates.

2. RESULTS AND DISCUSSION

2.1. Biomass Hydrolysates and Sample Summary. The contents of acetic acid, furfural, and HMF in 60 biomass hydrolysate samples determined by the HPLC method are listed in Table 3. Acetic acid, furfural, and HMF contents ranged from 1.58 to 5.00, 0.26 to 8.47, and 0.06 to 2.67 mg/mL with SDs of 0.90, 2.21, and 0.68, respectively. In the calibration set, acetic acid, furfural, and HMF contents ranged from 1.64 to 5.00, 0.26 to 8.47, and 0.06 to 2.67 mg/mL with SDs of 0.87, 2.32, and 0.75, respectively. In the validation set, acetic acid, furfural, and HMF contents ranged from 1.58 to 4.89, 0.70 to 7.02, and 0.07 to 1.77 mg/mL with SDs of 1.15, 2.18, and 0.56, respectively. The ranges, means, and SDs of acetic acid, furfural, and HMF contents in the calibration set covered those in the validation set, and both subsets showed consistent distributions, which are desired for model construction.

2.2. Biomass Hydrolysate Near-Infrared Spectra. The NIR spectra of 60 biomass hydrolysate samples with the full range of 10 000−4000 cm^{-1} are shown in Figure 1. The main absorbance regions were observed in the wavenumber ranges of 9000−8000, 7200−6200, and 5500−4000 cm^{-1}, which represent the overlap of several C−H second overtones, the O−H first stretch of H_2O, and the overlap of several C−H first stretch overtones, respectively.[28,38]

2.3. NIR Model Development. The full range (10 000−4000 cm^{-1}) of NIR spectra was first investigated for model development of acetic acid, furfural, and HMF contents. The regression coefficients (Figure 2) showed spikes around the very strong absorbance caused by O−H overtones around 7200 and 5400 cm^{-1}, and wavenumber ranges of less than 5000 cm^{-1} and more than 9000 cm^{-1} did not have large contribution to model development. Thus, these regions were excluded from some subsequent models. Three reduced wavenumber ranges (9000−5000; 9000−8000 and 7000−5000; and 7000−5000) of NIR spectra were used to optimize the prediction model performance. The results are shown in Table 4.

2.3.1. Acetic Acid. From the results shown in Table 4, the model developed using the full wavenumber range (10 000−4000 cm^{-1}) of spectra for acetic acid in the calibration set had an R^2 (cal.) of 0.90, RMSEC of 0.27, RPD of 2.5, and R^2 (val.) of 0.81. The reduced wavenumber range 1 (9000−5000 cm^{-1}) increased the R^2 (val.) of the model from 0.81 to 0.90 but R^2 (cal.) decreased from 0.90 to 0.67 because of the decreasing number of factors used for calibration. Although the model with the reduced wavenumber range 3 (7000−5000 cm^{-1}) had a high R^2 (cal.) of 0.94 and a low RMSEC of 0.22, the excessive

Table 2. Chemical Composition of Raw Biomass Used in this Experiment

biomass	cellulose (%, db[a])	hemicellulose (%, db[a])	lignin (%, db[a])	ash (%, db[a])	extractives (%, db[a])	moisture (%)
corn stover	30.61	24.04	11.33	1.61	27.22	4.14
switchgrass	32.72	28.81	16.78	0.89	17.48	3.77
sorghum	33.78	28.24	16.97	1.17	15.14	3.07
miscanthus	34.63	28.72	16.94	0.77	15.48	3.54

[a]db = dry basis.

DOI: 10.1021/acsomega.8b00636
ACS Omega 2018, 3, 5355−5361

Table 3. Statistics of Acetic Acid, Furfural, and HMF Contents Determined by the HPLC Method (Unit: mg/mL)[a,b]

	full set			calibration set			validation set		
analytes	range	mean	SD	range	mean	SD	range	mean	SD
acetic acid	1.58−5.00	3.37	0.90	1.64−5.00	3.37	0.87	1.58−4.89	3.51	1.15
furfural	0.26−8.47	3.58	2.21	0.26−8.47	3.66	2.32	0.70−7.02	3.65	2.18
HMF	0.06−2.67	0.68	0.68	0.06−2.67	0.70	0.75	0.07−1.77	0.79	0.56

[a]Full set has 60 samples, 50 of which are used for the calibration set and 10 of which are used for the validation set. [b]SD = standard deviation.

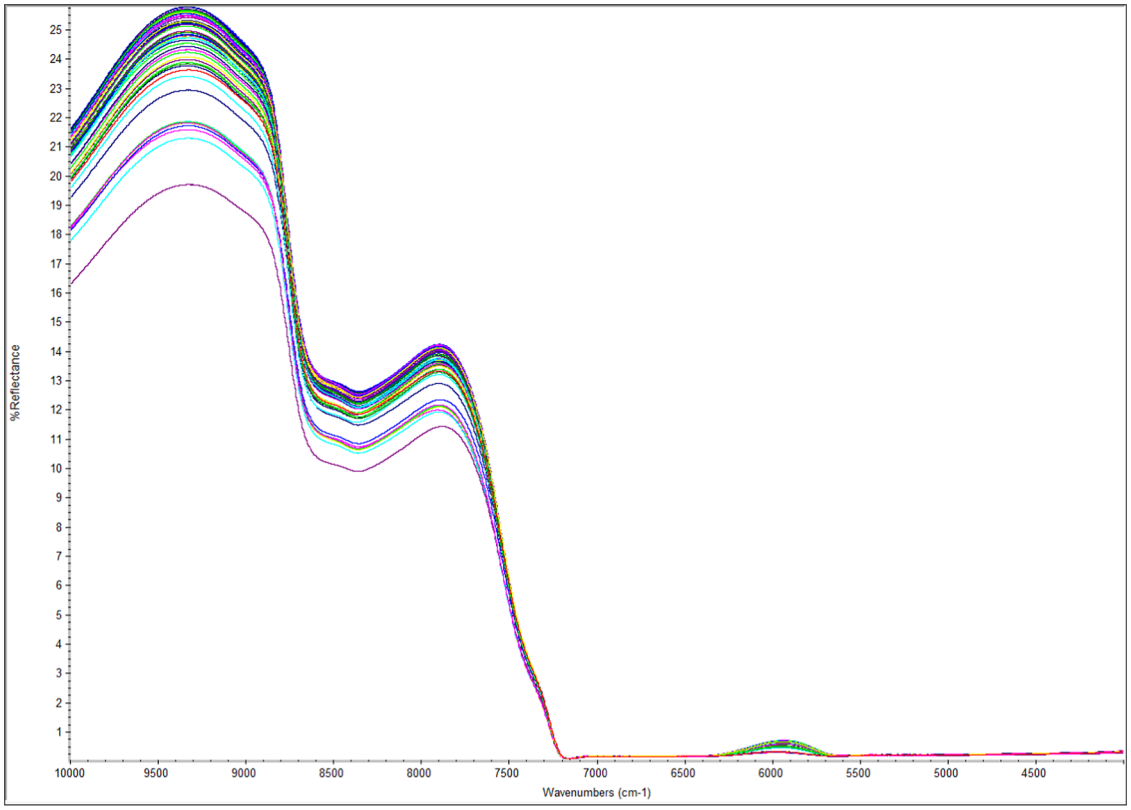

Figure 1. Averaged near-infrared (NIR) spectra of 60 biomass hydrolysates with 16 scans at a resolution of 8 cm^{-1}.

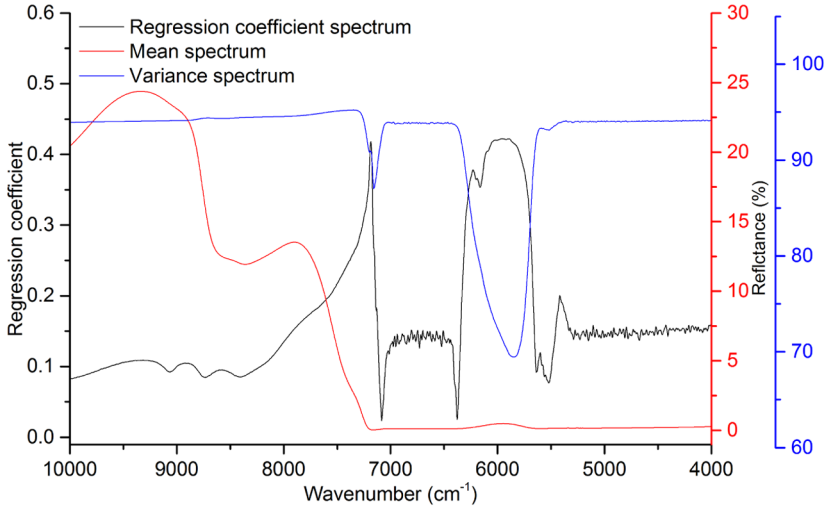

Figure 2. Regression coefficient, mean, and variance spectra of biomass hydrolysates in the partial least-square (PLS) model.

reduction of the wavenumber range resulted in the partial loss of key information of acetic acid when compared with the full wavenumber range, causing the decrease of R^2 (val.) from 0.81 to 0.73 and the increase of RMSEP from 0.46 to 0.56. Thus, the model using the reduced wavenumber range 3 did not show a good prediction ability for acetic acid contents. On the basis of the previously mentioned analysis, a reduced wavenumber range 2 (9000−8000 and 7000−5000 cm^{-1}) was generated by

DOI: 10.1021/acsomega.8b00636
ACS Omega 2018, 3, 5355−5361

Table 4. Model Development for Acetic Acid, Furfural, and HMF Prediction Using Different Wavenumber Ranges[a]

			wavenumber range			
analytes	analysis methods	evaluation index	full	reduced 1	reduced 2	reduced 3
acetic acid	PLS	R^2, cal.	0.90	0.67	0.96	0.94
		R^2, val.	0.81	0.90	0.85	0.73
		RMSEC	0.27	0.50	0.18	0.22
		RMSEP	0.46	0.43	0.43	0.56
		RPD	2.52	2.66	2.69	2.04
		factor used	10	7	10	8
furfural	PLS	R^2, cal.	0.99	0.99	0.99	0.99
		R^2, val.	0.97	0.98	0.99	0.99
		RMSEC	0.22	0.19	0.14	0.07
		RMSEP	0.54	0.48	0.28	0.30
		RPD	4.06	4.58	7.84	7.22
		factor used	10	10	9	9
HMF	PLS	R^2, cal.	0.87	0.87	0.90	0.92
		R^2, val.	0.93	0.93	0.94	0.92
		RMSEC	0.24	0.24	0.21	0.19
		RMSEP	0.19	0.19	0.20	0.23
		RPD	2.95	3.0	2.76	2.47
		factor used	8	8	7	7

[a]Full wavenumber range: 10 000−4000 cm^{-1}; reduced wavenumber range 1: 9000−5000 cm^{-1}; reduced wavenumber range 2: 9000−8000 and 7000−5000 cm^{-1}; reduced wavenumber range 3: 7000−5000 cm^{-1}; R^2, cal.: determination coefficient of calibration set; R^2, val.: determination coefficient of validation set; RMSEC: root-mean-square error of calibration; RMSEP: root-mean-square error of prediction; RPD: ratio of standard deviation of the reference values to the RMSEP.

further compressing the reduced range 1 and extending the reduced range 3. The wavenumber range of 8000−7000 cm^{-1} was excluded because it was mainly attributed to sugars and it contains noise caused by the very strong absorbance of the O−H overtone.[28] Results showed that the model with the reduced wavenumber range 2 had the best calibration and prediction performance with an R^2 (cal.) of 0.96, R^2 (val.) of 0.85, RMSEC of 0.18, RMSEP of 0.43, and RPD of 2.7.

2.3.2. Furfural. The full wavenumber range was first used to develop the model of furfural, and the results are listed in Table 4. The first model of furfural showed an R^2 (cal.) of 0.99, R^2 (val.) of 0.97, RMSEC of 0.22, RMSEP of 0.54, and RPD of 4.1, indicating a fair prediction performance for furfural contents. Also, as the wavenumber range used to develop the model of furfural was reduced from the full range to reduced ranges 1 and 2, both R^2 (cal.) and R^2 (val.) further increased as well as RPD and both RMSEC and RMSEP further decreased as well as the number of factors used, demonstrating that the optimization of the wavenumber range further improved the prediction model performance for furfural contents. However, when the reduced range 2 was further compressed to the reduced range 3, neither R^2 (cal.) nor R^2 (val.) increased, RMSEP increased, and RPD decreased, indicating that the excessive reduction of the wavenumber range also caused the partial loss of key information of furfural when compared with the other models that used reduced wavenumber ranges. Thus, the model developed on wavenumber range 2 was chosen to predict the contents of furfural.

2.3.3. HMF. The full wavenumber range was used to develop the model to predict HMF, and the results are listed in Table 4. The first model of HMF showed an R^2 (cal.) of 0.87, R^2 (val.) of 0.93, RMSEC of 0.24, RMSEP of 0.19, and RPD of 3.0. The model performances, especially the calibration performance, of HMF were not as good as those of furfural. From the models developed using the reduced wavenumber ranges, results were generally similar to those from the full wavenumber model with no model showing consistent improvement over the full model. The reduced wavenumber range 2 model did have slightly better R^2 (val.) and was chosen as the best model.

On the basis of the previously mentioned analysis, the reduced wavenumber range 2 (9000−8000 and 7000−5000 cm^{-1}) was finally employed to develop the prediction models for acetic acid, furfural, and HMF contents. Spectrum outlier diagnostics showed that the distances of all data points were less than 3.0 (data not shown) and suggested that no outlier existed in the spectra of samples. Figure 3 shows the plot of predicted versus actual values in the optimized model with good correlation coefficients of 0.98 (cal.) and 0.92 (val.) for acetic acid, 0.99 (cal.) and 0.99 (val.) for furfural, and 0.95 (cal.) and 0.97 (val.) for HMF. Figure 3 also shows that predicted versus actual contents of acetic acid, furfural, and HMF were randomly distributed, further confirming the good performance of the prediction models.

3. CONCLUSIONS

The NIRS prediction models for rapid and accurate analysis of acetic acid, furfural, and HMF contents in biomass hydrolysates were developed successfully, which shows that this can be a simple and rapid method for the industrial application of ethanol production. The model optimized on the reduced range 2 (9000−8000 and 7000−5000 cm^{-1}) generally had a better overall performance for the prediction of acetic acid, furfural, and HMF contents than that of the model developed on the full wavenumber range (10 000−4000 cm^{-1}) in terms of R^2 (cal.), R^2 (val.), RMSEC, RMSEP, and RPD. The NIR method can predict acetic acid, furfural, and HMF in biomass hydrolysates in <1 min and has no cost for reagents.

4. EXPERIMENTAL SECTION

4.1. Chemicals and Materials. Furfural (purity > 98%) and HMF (purity > 97%) were purchased from Sigma-Aldrich (St. Louis, MO). Ultrapure water (HPLC grade), acetic acid

DOI: 10.1021/acsomega.8b00636
ACS Omega 2018, 3, 5355−5361

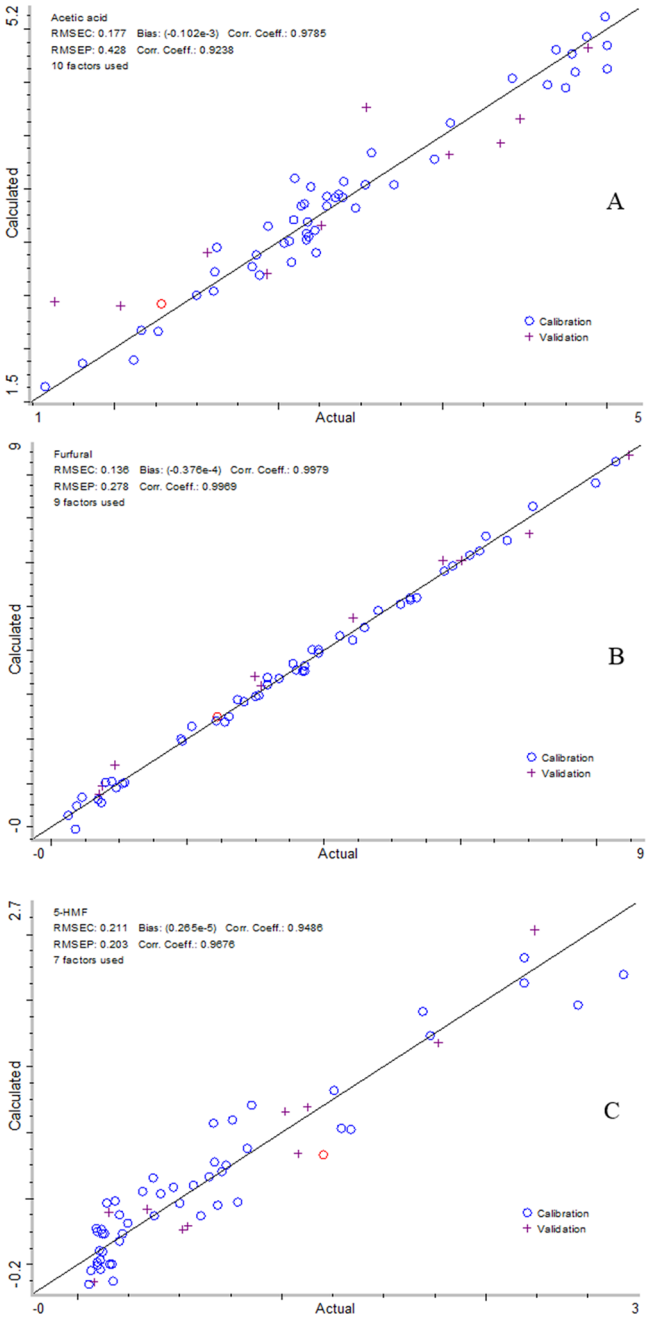

Figure 3. Linear regression plots of calculated versus actual acetic acid (A), furfural (B), and HMF (C).

(HPLC grade), and sulfuric acid were purchased from Thermo Fisher Scientific Chemicals Inc. (Ward Hill, MA). Corn stover, switchgrass, sorghum, and miscanthus were harvested from the Kansas State University Research Farm (Manhattan, KS). After harvest, biomass samples were air-dried at 60 °C for at least 1 week, ground to <1 mm particle size using a SM 2000 cutting mill (Retsch Inc. Newton, PA) and then sealed in plastic bags with zippers and stored at room temperature before use.

4.2. Biomass Pretreatment and Biomass Hydrolysate Collection. Five grams of ground biomass with 50 mL of distilled water or dilute sulfuric acid solution was weighed into a 75 mL stainless steel reactor (Swagelok, Kansas City Valve & Fitting Co., KS) made of 316L stainless steel with a measured internal volume of 75 mL (outside diameter of 38.1 mm, length of 125 mm, and wall thickness of 2.4 mm). When the sand bath (Techne, Inc., Princeton, NJ) reached a designated temperature (Table 1), the reactor was submerged into the sand bath for different reaction times (Table 1). Once the reaction time was complete, the reactor was submerged in ice water to quench the hydrolysis reaction. Biomass slurry was filtrated to collect biomass hydrolysates (liquid fraction of biomass slurry). After that, the biomass hydrolysate was placed in a freezer until analysis. The biomass residue was washed with 100 mL of distilled water to remove degradation products attached on the surface of the biomass residue and then dried at 45 °C for 24 h in preparation for further analysis. Four types of biomass (corn stover, switchgrass, sorghum, and miscanthus) were used in this experiment. Table 2 shows their chemical compositions measured by the NREL standard procedure.[39] Cellulose, hemicellulose, lignin, ash, extractives, and moisture contents ranged from 30.61 to 34.63, 24.04 to 28.81, 11.33 to 16.97, 0.77 to 1.61, 15.14 to 27.22, and 3.07 to 4.14%, respectively. To reduce prediction biases and limits of the NIRS prediction models, a wide range of biomass hydrolysate samples were prepared with different pretreatment conditions (Table 1). The ranges of temperature, time, and acid concentration were 120−230 °C, 10−60 min, and 0−5%, respectively. After pretreatment, 60 biomass hydrolysate samples were collected by vacuum filtration for both HPLC and NIRS measurements.

4.3. HPLC Analysis of Furfural, HMF, and Acetic Acid. Furfural, HMF, and acetic acid in biomass hydrolysates were determined by the NREL method "Determination of Sugars, Byproducts, and Degradation Products in Liquid Fraction Process Samples". The HPLC spectra were recorded with a G1362A refractive index detector (RID) (Agilent, Santa Clara, CA) and an Aminex HPX-87H ion exchange column (7.8 × 300 mm, Bio-Rad). The injection volume for each of the samples was 20 μL; the mobile phase was 0.005 M sulfuric acid water with a flow rate of 0.6 mL/min; and the column oven and RID were set at 60 and 45 °C, respectively. The mobile phase was degassed for 15 min by a P250D ultrasonic apparatus (ETL testing laboratories, Inc., Cortland, NY) before use. Compounds were identified by comparing their retention times to those of standards. Data were acquired and processed using OpenLAB CDS C.01.05 ChemStation (Agilent, Santa Clara, CA).

4.4. NIR Scans of Biomass Hydrolysates. The NIR spectra of biomass hydrolysates were recorded in absorbance mode using an Antaris II FT-NIR analyzer with an automated transmission sampling module (Thermo Fisher Scientific Inc., Madison, WI). A total of 1.2 mL of each biomass hydrolysate was loaded into a 2 mL round sample tube used for the NIR measurement of liquid samples with air as the blank. A blank scan was performed before each sample was scanned. No delay time was set before both blank and sample scans. The spectra of each sample were averaged with 16 scans at a resolution of 8 cm^{-1} in the wavenumber range of 10 000−4000 cm^{-1}. Attenuator and gain were set at B screen (attenuate 6−10% of incident light transmitted) and 8 times, respectively, using the automatic optimization function of the FT-NIR instrument to analyze the representative biomass hydrolysate. The aperture was used to focus the light beam to completely pass through each sample.

4.5. Spectral Processing and Chemometric Analysis. Both spectral processing and chemometric analysis were performed by TQ Analyst 8.6.12 software (Thermo Fisher Scientific Inc., Madison, WI). The path length type was set at

DOI: 10.1021/acsomega.8b00636
ACS Omega 2018, 3, 5355−5361

constant on the basis of the fact that sample cells have a fixed path length and biomass hydrolysates are homogeneous liquids. To reduce the random noise and improve the signal-to-noise ratio and the model robustness, Savitzky−Golay smoothing was used to reduce the noise of the original NIR spectra.[5] In addition, the wavenumber range of the NIR spectra was reduced to improve the performance of prediction models.

A total of 60 biomass hydrolysates were sequenced in a descending order according to the measured value of furfural. One in every six samples was assigned randomly to the validation set with a total of 10 samples, and the remaining 50 samples were used for the calibration set to develop prediction models. The full wavenumber range from 10 000 to 4000 cm^{-1} was used unless otherwise specified. A partial least-squares (PLSs) regression was used to obtain the relationship between the reference and NIR spectra.

Prediction models were evaluated according to the R^2 and RPD values. R^2 values in the range of 0.50−0.65, 0.66−0.81, 0.82−0.90, and 0.91−1.00 indicated that models were adequate, fair, good, and excellent, respectively.[40] The RPD considers the effect of both RMSEP and data variation. The values of RPD of <2.3, 2.4−3.0, 3.1−4.9, 5−6.4, and 6.5−8.0 and >8.0 indicated very poor, poor, fair, good, very good, and excellent prediction of the model developed, respectively.[41] To reduce the possibility of overfitting caused by the addition of excess factors to reach a minimum prediction error, the prediction residual error sum of squares was used to select the optimal number of factors for the model calibration. The Chauvenet test was also used to eliminate outliers defined as the points at distances in the principal component space greater than 3.0.

AUTHOR INFORMATION

Corresponding Authors

*E-mail: Floyd.Dowell@ARS.USDA.GOV. Tel.: 785-776-2753 (F.D.).

*E-mail: dwang@ksu.edu. Tel.: 785-532-2919. Fax: 785-532-5825 (D.W.).

ORCID

Donghai Wang: 0000-0001-9293-1387

Notes

The authors declare no competing financial interest.

ACKNOWLEDGMENTS

This study is partially supported by the U.S. National Science Foundation through Award 1562671. This is contribution No. 18-172-J of the Kansas Agricultural Experiment Station. Mention of trade names or commercial products in this publication is solely for the purpose of providing specific information and does not imply recommendation or endorsement by the U.S. Department of Agriculture. USDA is an equal opportunity provider and employer.

REFERENCES

(1) Sasmal, S.; Goud, V. V.; Mohanty, K. Ultrasound assisted lime pretreatment of lignocellulosic biomass toward bioethanol production. *Energy Fuels* **2012**, *26*, 3777−3784.

(2) Xu, Y.; Wang, D. Integrating starchy substrate into cellulosic ethanol production to boost ethanol titers and yields. *Appl. Energy* **2017**, *195*, 196−203.

(3) Naik, S. N.; Goud, V. V.; Rout, P. K.; Dalai, A. K. Production of first and second generation biofuels: a comprehensive review. *Renewable Sustainable Energy Rev.* **2010**, *14*, 578−597.

(4) Hasegawa, I.; Tabata, K.; Okuma, O.; Mae, K. New pretreatment methods combining a hot water treatment and water/acetone extraction for thermo-chemical conversion of biomass. *Energy Fuels* **2004**, *18*, 755−760.

(5) Zhang, K.; Zhou, L.; Brady, M.; Xu, F.; Yu, J.; Wang, D. Fast analysis of high heating value and elemental compositions of sorghum biomass using near-infrared spectroscopy. *Energy* **2017**, *118*, 1353−1360.

(6) Mosier, N.; Wyman, C.; Dale, B.; Elander, R.; Lee, Y. Y.; Holtzapple, M.; Ladisch, M. Features of promising technologies for pretreatment of lignocellulosic biomass. *Bioresour. Technol.* **2005**, *96*, 673−686.

(7) Pu, Y.; Hu, F.; Huang, F.; Davison, B. H.; Ragauskas, A. J. Assessing the molecular structure basis for biomass recalcitrance during dilute acid and hydrothermal pretreatments. *Biotechnol. Biofuels* **2013**, *6*, 15.

(8) Wang, Z.; Cheng, J. Lime pretreatment of coastal bermudagrass for bioethanol production. *Energy Fuels* **2011**, *25*, 1830−1836.

(9) Kim, Y.; Kreke, T.; Ko, J. K.; Ladisch, M. R. Hydrolysis-determining substrate characteristics in liquid hot water pretreated hardwood. *Biotechnol. Bioeng.* **2015**, *112*, 677−687.

(10) Li, H.; Pu, Y.; Kumar, R.; Ragauskas, A. J.; Wyman, C. E. Investigation of lignin deposition on cellulose during hydrothermal pretreatment, its effect on cellulose hydrolysis, and underlying mechanisms. *Biotechnol. Bioeng.* **2014**, *111*, 485−92.

(11) Zheng, Y.; Lee, C.; Yu, C.; Cheng, Y.; Zhang, R.; Jenkins, B. M.; VanderGheynst, J. S. Dilute acid pretreatment and fermentation of sugar beet pulp to ethanol. *Appl. Energy* **2013**, *105*, 1−7.

(12) Jeong, S. Y.; Lee, J. W. Hydrothermal Treatment. In *Pretreatment of Biomass: Processes and Technologies*, 1st ed.; Pandy, A., Negi, S., Binod, P., Larroche, C., Eds.; Academic Press, 2015; pp 61−74.

(13) Chandel, A. K.; Silva, S. S. D.; Singh, O. V. Detoxification of lignocellulose hydrolysates: biochemical and metabolic engineering toward white biotechnology. *BioEnergy Res.* **2013**, *6*, 388−401.

(14) Chheda, J. N.; Roman-Leshkov, Y.; Dumesic, J. A. Production of 5-hydroxymethylfurfural and furfural by dehydration of biomass-derived mono-and poly-saccharides. *Green Chem.* **2007**, *9*, 342−350.

(15) Klinke, H. B.; Thomsen, A. B.; Ahring, B. K. Inhibition of ethanol-producing yeast and bacteria by degradation products produced during pre-treatment of biomass. *Appl. Microbiol. Biotechnol.* **2004**, *66*, 10−26.

(16) Sluiter, A.; Hames, B.; Ruiz, R.; Scarlata, C.; Sluiter, J.; Templeton, D. *Determination of Sugars, Byproducts, and Degradation Products in Liquid Fraction Process Samples*; Technical Report NREL/TP-510-42623; Renewable Energy Laboratory, 2006.

(17) Chi, C.; Zhang, Z.; Chang, H.; Jameel, H. Determination of furfural and hydroxymethylfurfural formed from biomass under acidic conditions. *J. Wood Chem. Technol.* **2009**, *29*, 265−276.

(18) Davies, S. M.; Linforth, R. S.; Wilkinson, S. J.; Smart, K. A.; Cook, D. J. Rapid analysis of formic acid, acetic acid, and furfural in pretreated wheat straw hydrolysates and ethanol in a bioethanol fermentation using atmospheric pressure chemical ionisation mass spectrometry. *Biotechnol. Biofuels* **2011**, *4*, 28.

(19) Dong, B. Y.; Chen, Y.; Zhao, C.; Zhang, S.; Guo, X.; Xiao, D. Simultaneous determination of furfural, acetic acid, and 5-hydroxymethylfurfural in corncob hydrolysates using liquid chromatography with ultraviolet detection. *J. AOAC Int.* **2013**, *96*, 1239−1244.

(20) Liu, X.; Ai, N.; Zhang, H.; Lu, M.; Ji, D.; Yu, F.; Ji, J. Quantification of glucose, xylose, arabinose, furfural, and HMF in corncob hydrolysate by HPLC-PDA−ELSD. *Carbohydr. Res.* **2012**, *353*, 111−114.

(21) Li, H.; Chai, X.; Zhan, H.; Fu, S. Rapid determination of furfural in biomass hydrolysate by full evaporation headspace gas chromatography. *J. Chromatogr. A* **2010**, *1217*, 7616−7619.

(22) Li, J.; Xu, Y.; Zhang, M.; Wang, D. Determination of furfural and 5-hydroxymethylfurfural in biomass hydrolysate by high-performance liquid chromatography. *Energy Fuels* **2017**, *31*, 13769−13774.

DOI: 10.1021/acsomega.8b00636
ACS Omega 2018, 3, 5355−5361

(23) Fagan, C. C.; O'Donnell, C. P.; O'Callaghan, D. J.; Downey, G.; Sheehan, E. M.; Delahunty, C. M.; Everard, C.; Guinee, T. P.; Howard, V. Application of Mid-Infrared Spectroscopy to the Prediction of Maturity and Sensory Texture Attributes of Cheddar Cheese. *J. Food Sci.* **2007**, *72*, E130−E137.
(24) Gowen, A. A.; Tsenkova, R.; Esquerre, C.; Downey, G.; O'Donnell, C. P. Use of near infrared hyperspectral imaging to identify water matrix co-ordinates in mushrooms (Agaricus bisporus) subjected to mechanical vibration. *J. Near Infrared Spectrosc.* **2009**, *17*, 363−371.
(25) Gowen, A. A.; O'Donnell, C. P.; Taghizadeh, M.; Cullen, P. J.; Frias, J. M.; Downey, G. Hyperspectral imaging combined with principal component analysis for bruise damage detection on white mushrooms (Agaricus bisporus). *J. Chemom.* **2008**, *22*, 259−267.
(26) Herkert, T.; Prinz, H.; Kovar, K. A. One hundred percent online identity check of pharmaceutical products by near-infrared spectroscopy on the packaging line. *Eur. J. Pharm. Biopharm.* **2001**, *51*, 9−16.
(27) Reich, G. Near-infrared spectroscopy and imaging: basic principles and pharmaceutical applications. *Adv. Drug Delivery Rev.* **2005**, *57*, 1109−1143.
(28) Xu, F.; Wang, D. Rapid determination of sugar content in corn stover hydrolysates using near infrared spectroscopy. *Bioresour. Technol.* **2013**, *147*, 293−298.
(29) Hayes, D. J. Development of near infrared spectroscopy models for the quantitative prediction of the lignocellulosic components of wet Miscanthus samples. *Bioresour. Technol.* **2012**, *119*, 393−405.
(30) He, W.; Hu, H. Prediction of hot-water-soluble extractive, pentosan and cellulose content of various wood species using FT-NIR spectroscopy. *Bioresour. Technol.* **2013**, *140*, 299−305.
(31) Nkansah, K.; Dawson-Andoh, B.; Slahor, J. Rapid characterization of biomass using near infrared spectroscopy coupled with multivariate data analysis: Part 1 yellow-poplar (*Liriodendron tulipifera* L.). *Bioresour. Technol.* **2010**, *101*, 4570−4576.
(32) Wolfrum, E. J.; Sluiter, A. D. Improved multivariate calibration models for corn stover feedstock and dilute-acid pretreated corn stover. *Cellulose* **2009**, *16*, 567−576.
(33) Xu, F.; Zhou, L.; Zhang, K.; Yu, J.; Wang, D. Rapid determination of both structural polysaccharides and soluble sugars in sorghum biomass using near-infrared spectroscopy. *BioEnergy Res.* **2015**, *8*, 130−136.
(34) Zhang, K.; Xu, Y.; Johnson, L.; Yuan, W.; Pei, Z.; Wang, D. Development of near-infrared spectroscopy models for quantitative determination of cellulose and hemicellulose contents of big bluestem. *Renewable Energy* **2017**, *109*, 101−109.
(35) Posom, J.; Sirisomboon, P. Evaluation of lower heating value and elemental composition of bamboo using near infrared spectroscopy. *Energy* **2017**, *121*, 147−158.
(36) Posom, J.; Shrestha, A.; Saechua, W.; Sirisomboon, P. Rapid non-destructive evaluation of moisture content and higher heating value of Leucaena leucocephala pellets using near infrared spectroscopy. *Energy* **2016**, *107*, 464−472.
(37) Mancini, M.; Rinnan, A.; Pizzi, A.; Toscano, G. Prediction of gross calorific value and ash content of woodchip samples by means of FT-NIR spectroscopy. *Fuel Process. Technol.* **2018**, *169*, 77−83.
(38) Shenk, J. S.; Workman, J.; Westerhaus, M. O. Application of NIR Spectroscopy to Agricultural Products. In *Handbook of Near-Infrared Analysis*, 3rd ed.; Burns, D., Ciurczak, E., Eds.; Marcel Dekker Inc: New York, 2001; pp 419−474.
(39) Sluiter, A.; Hames, B.; Ruiz, R.; Scarlata, C.; Sluiter, J.; Templeton, D.; Crocker, D. *Determination of Structural Carbohydrates and Lignin in Biomass*; Technical Report NREL/TP-510-42618; Renewable Energy Laboratory, 2008.
(40) Fagan, C. C.; Everard, C. D.; McDonnell, K. Prediction of moisture, calorific value, ash and carbon content of two dedicated bioenergy crops using near-infrared spectroscopy. *Bioresour. Technol.* **2011**, *102*, 5200−5206.
(41) Williams, P. C. Implementation of Near-Infrared Technology. In *Near-Infrared Technology in the Agricultural and Food Industries*, 2nd ed.; Williams, P. C., Norris, K. H., Eds.; American Association of Cereal Chemists: Minnesota, 2001; pp 145−169.

DOI: 10.1021/acsomega.8b00636
ACS Omega 2018, 3, 5355−5361